Published in final edited form as:
Neurogastroenterol Motil. 2010 April ; 22(4): 462–e110. doi:10.1111/j.1365-2982.2009.01435.x.

Lack of Serotonin 5-HT$_{2B}$ Receptor Alters Proliferation and Network Volume of Interstitial Cells of Cajal *in Vivo*

Vivek S. Tharayil[1], **Mira M. Wouters**[1,*], **Jennifer E. Stanich**[1], **Jaime L. Roeder**[1], **Sha Lei**[1], **Arthur Beyder**[1], **Pedro J. Gomez-Pinilla**[1], **Michael D. Gershon**[3], **Luc Maroteaux**[4], **Simon J. Gibbons**[1,2], and **Gianrico Farrugia**[1,2]

[1] Enteric Neuroscience Program, Miles and Shirley Fiterman Center for Digestive Diseases, Mayo Clinic, Rochester, MN, USA

[2] Dept of Physiology and Biomedical Engineering, Mayo Clinic, Rochester, MN, USA

[3] Department of Pathology and Cell Biology, Columbia University, New York, NY, USA

[4] INSERM, U839, Institut du Fer à Moulin, 17 rue du Fer à Moulin, 75005 Paris, France

Abstract

Background—Normal gastrointestinal motility requires intact networks of interstitial cells of Cajal (ICC). ICC numbers are maintained by a balance between cell loss factors and survival/trophic/growth factors. Activation of 5-HT$_{2B}$ receptors expressed on ICC increases ICC proliferation *in vitro*. It is not known whether 5-HT$_{2B}$ receptors on ICC are activated *in vivo*. The aims of this study were to investigate if adult ICC proliferate, whether the proliferation of ICC *in vivo* is affected by knocking out the 5-HT$_{2B}$ receptor, and if alterations in proliferation affect ICC networks.

Methods—Proliferating ICC were identified by immunoreactivity for Ki67 in both the myenteric and deep muscular plexus regions of the jejunum in mice with a targeted insertion of a neomycin resistance cassette into the second coding exon of the *htr2b* receptor gene.

Key Results—Adult ICC do proliferate. The number of proliferating ICC was lower in the myenteric plexus region of *Htr2b*$^{-/-}$ compared to *Htr2b*$^{+/+}$ mice. The volume of Kit-positive ICC was 30% lower in the myenteric plexus region and 40% lower in the deep muscular plexus region in *Htr2b*$^{-/-}$ mice where the number of ICC was also reduced.

Conclusions & Inferences—ICC proliferate in adult mice and activation of 5-HT$_{2B}$ receptors results in increased proliferation of ICC *in vivo*. Furthermore, lack of 5-HT$_{2B}$ receptor signaling reduces the density of ICC networks in mature mice. These data suggest that 5-HT$_{2B}$ receptor signaling is required for maintenance of ICC networks, adding 5-HT to the growing number of factors shown to regulate ICC networks.

Keywords

Cellular plasticity; Kit; Gastrointestinal motility; Mouse jejunum; Serotonin receptors

Send correspondence to: Gianrico Farrugia, MD, Mayo Clinic, 200 First Street SW, Rochester MN, 55905, Tel 507 284 4695, Fax 507 284 0266, farrugia.gianrico@mayo.edu.
*Current Address: Translational Research Center for Gastrointestinal Diseases, University of Leuven, Leuven, Belgium

Disclosures: The authors have no competing interests.

Introduction

Interstitial cells of Cajal (ICC) contribute to normal motility in the gastrointestinal tract. The role of ICC in motility is dependent on four properties of the cells. ICC generate the electrical slow wave.1, 2 ICC amplify nitrergic and cholinergic input from enteric nerves to smooth muscle.3, 4 ICC are mechanosensitive5, 6 and ICC set the membrane potential gradients across the muscle wall by generating carbon monoxide.7

Loss of ICC is associated with a number of gastrointestinal motility disorders including diabetic gastroparesis8 and slow transit constipation.9, 10 ICC networks are not static, rather there is a constant turnover of ICC networks, even in the absence of disease.11–13 Therefore, there is considerable interest in understanding the factors that regulate the development, maintenance and loss of ICC in health and disease. The best characterized growth factor for ICC is stem cell factor, which binds to the Kit receptor tyrosine kinase.14 Other factors that affect the survival of ICC *in vitro* and *in vivo* include insulin-like growth factor 1,15 nitric oxide,16 levels of oxidative stress17 and serotonin (5-hydroxytryptamine, 5-HT).18 The mechanisms by which these factors support ICC include altering stem cell factor availability19 or directly altering replacement, survival or loss of ICC.11

Serotonin is a neuro-humoral factor present in large quantities in the gastrointestinal tract.20 Serotonin alters motility through activation of receptors found on several cell types in the muscularis propria. In other tissues, serotonin is also known to regulate proliferation and survival of cells by activating 5-HT_{1A}, 5-HT_{1D}, 5-HT_{2B} or 5-HT_{2C} receptors.21–27 In the gastrointestinal tract, only the 5-HT_{2B} receptor has been linked to the regulation of enteric neuron survival28 and ICC proliferation.18 These effects are congruent with data showing that 5-HT_{2B} receptors are involved in cell differentiation and proliferation in mouse hepatocytes and cardiomyocytes and retinal cells in Xenopus.25–27

We have recently shown that 5-HT_{2B} receptors are expressed on ICC in adult mice and that activation of these receptors increases proliferation of ICC cultured from neonatal mouse jejunum.18 Most 5-HT in the gut is produced by enterochromaffin cells29, 30 and is rapidly taken up or metabolized by neighboring cells. The other source of serotonin is from descending interneurons.31, 32 It is therefore not known if the 5-HT_{2B} receptor on ICC is actually activated *in vivo* and whether the degree of activation is sufficient to alter ICC networks. Therefore, we investigated the changes in ICC network volume, ICC number and rates of ICC proliferation in the jejunal smooth muscle of adult mice that have a targeted insertion of a neomycin resistance cassette into the second coding exon of the *htr2b* receptor gene33 and their wild type controls. In these transgenic mice, there is complete knockout of the 5-HT_{2B} receptor protein, which results in cardiac malformations due to decreased 5-HT-mediated regulation of cell proliferation.33 Effects of 5-HT_{2B} receptor knockout on cells in the gastrointestinal tract have not been previously reported.

Materials and Methods

Animals

Mice were maintained and experiments performed as approved by the Institutional Animal Care and Use Committee (IACUC) of the Mayo Clinic. Mice homozygous for knockout of *Htr2b* gene expression were received from Dr. Michael D. Gershon, Columbia University Medical Center, New York in collaboration with Dr. Luc Maroteaux, who generated the original mice. The *Htr2b*$^{-/-}$ mice were back-crossed to B6129SF2 wild type mice (Jackson Laboratory, Bar Harbor ME) to produce a colony of *Htr2b*$^{+/-}$ mice from which the knockout and control animals for this study were obtained. The mice used for the whole mount experiments were of 4 weeks of age. These mice were fully weaned and were on adult diets.

Previous reports have established that ICC networks in mice reach their mature density and distribution by 15 days of age.34 The four week old mice were killed by CO_2 inhalation. The jejunum was quickly dissected out, flushed with ice-cold, calcium-free Hanks balanced salt solution (Invitrogen, Carlsbad, CA) and pinned onto a sylgard lined petri dish. Approximately 1 cm^2 of the muscle layer from the jejunum was taken for whole mount staining. For primary ICC cultures, 2–4 day old pups were killed by CO_2 inhalation and cervical dislocation. The jejunum was quickly dissected out, flushed with ice-cold, calcium-free Hanks balanced salt solution, pinned onto a sylgard lined Petri dish and the mucosa and mesentery dissected out.

Laser Capture Microdissection

Four week old *Htr2b*$^{-/-}$ and *Htr2b*$^{+/+}$ control mice were used for these experiment. The experiments were done under strict RNAse free conditions. Small intestines were dissected out and 8 μm sections were mounted on Fischer brand Superfrost Plus microscope glass slides (Fischer Scientific, Pittsburgh PA) and stored at −80°C. The slides with the tissue were then thawed for 30 seconds and dehydrated in alcohol and xylene. The small intestinal fresh frozen sections were stained using the HistoGene™ LCM Frozen Section Staining Kit (Arcturus Bioscience Inc., Mountain View, CA). The slides were then placed in a dessicator with fresh dessicant and each slide was taken individually for Veritas laser capture microdissection (Arcturus Bioscience Inc.). After the cells from the circular muscle and DMP region were captured using the Capsure Macro LCM caps (Arcturus Bioscience Inc.), they were inserted into a 0.5 mL microcentrifuge tube (Applied BioSystems) containing 50 μL of Extraction Buffer. The CapSure cap-microcentrifuge tube assembly was then inverted to ensure that the extraction buffer was covering the CapSure Macro LCM cap. It was then incubated for 30 minutes at 42°C and then centrifuged at 800 xg for 2 minutes to collect the cell extract into the microcentrifuge tube.

RNA Isolation

The cell extract collected by LCM was then used for RNA isolation using the PicoPure RNA Isolation Kit (Arcturus Bioscience Inc.) and following the protocol as described by the manufacturer.

Reverse Transcription - Polymerase Chain Reaction

To determine the expression of $5HT_{2B}$ receptor in adult mouse jejunal tissue obtained from LCM and in adult mouse brain, polymerase chain reaction (PCR) was performed using the GeneAmp Gold RNA PCR reagent Kit (Applied Biosystems). Adult mouse brain served as positive control. Twenty five μL PCR reactions were set up (95°C for 10 min, 35 times 94°C for 20 sec, Melting Temp Tm for 30 sec, 72°C for Extension time (Ext.T) and 72°C for 7 min). One μL of the first PCR reaction was used for the nested PCR (95°C for 10 min, 35 times 94°C for 20 sec, Tm for 30 sec, 72°C for Ext.T, 72°C for 7 min). The optimized PCR programs are reported in Table 1.

Whole mount staining

All whole mount labeling procedures were done at 4 °C. After rinsing the tissue with cold phosphate buffered saline (PBS, 0.1M), the tissue was acetone-fixed and rinsed again with PBS before being incubated with 10% Normal Donkey Serum (NDS) (Jackson Immunoresearch Laboratories, West Grove, PA) and 0.2% Triton-X-100 (Sigma) in PBS for 1 hr to minimize non-specific antibody binding. The tissue was incubated overnight with the rat monoclonal anti-c-Kit antibody, ACK2 (eBioscience, San Diego, CA) at 1.65 μg mL-1 in 5% NDS. Tissues were then post fixed with 4% paraformaldehyde for 30 min, rinsed again with PBS, and incubated with a rabbit polyclonal antibody to the proliferation marker, Ki67

(Novus Biologicals, Littleton, CO) at 3 μg mL-1 in 5% NDS for 6hrs. Next, the tissues were rinsed in 1X PBS and incubated overnight with secondary antibodies, donkey anti-rat IgG conjugated to Cy3 (1.8 μg mL-1, in 2.5% NDS; Jackson Immunoresearch Laboratories) and donkey anti-rabbit IgG conjugated to Cy5 (7.5 μg mL-1, in 2.5% NDS; Jackson Immunoresearch Laboratories) in the dark. After overnight staining, the tissue was washed with PBS and incubated for 30 min in 4′, 6-diamidino-2-phenylindole (DAPI, 0.01 μg mL-1 in dH2O; Invitrogen, Carlsbad, CA) as a nuclear counter stain, and the whole mounts mounted with slow fade (Invitrogen, Carlsbad, CA).

Confocal Microscopy

Images of the labeled whole mounts were collected by laser scanning confocal microscopy (LSM 5, Zeiss, Oberkochen, Germany and Olympus FV 1000, Olympus America Inc., Center Valley, PA). ICC were identified by Kit immunoreactivity and the presence of 2 or more cellular processes. Proliferating ICC were identified by immunoreactivity for Ki67 that co-localized with the DAPI signal and that was enclosed by Kit positive membrane structures. To count proliferation, we examined 168 stacks each from *Htr2b*$^{+/+}$ and *Htr2b*$^{-/-}$ mice. To measure the ICC volume and count the total number of ICC deep muscular plexus (ICC-DMP), we used a total of 84 stacks each from *Htr2b*$^{+/+}$ and *Htr2b*$^{-/-}$ mice. The images were collected using a 40X 1.2 NA water immersion objective from Zeiss and a 40X 1.30 NA oil immersion objective from Olympus. The optimal z axis step for each objective was set by using an Airey number of 1 for the excitation wavelength of Cy5 (633 nm). We adjusted the settings on the confocal microscope to collect data from the full range of positively labeled voxels in the field. We also carefully picked the thresholds for segmentation of the images so that the finer, less bright processes are not fragmented by segmentation and all of the labeled voxels are represented in the binary map of the labeled voxels. We collected images from the same field repeatedly to bleach out the signal and confirmed that even when the image was dimmer, the thresholding method reported the same image volume.

Due to slight differences in the field size between the images collected with the two confocal microscopes, the number of dividing ICC in each stack of confocal images was divided by the field size (XY dimensions) of each stack to give the number of ICC in the whole thickness of a 1 mm^2 area of the muscle. ICC-DMP were counted separately. They were identified by their location on the submucosal side of the circular muscle layer and by morphology. ICC-DMP were Kit positive, had clear processes and a DAPI-labeled nucleus. The total number of ICC-DMP across the deep muscular plexus region in each stack was normalized, as explained above for dividing ICC, to an area of 1mm^2. The images were also examined to determine the thickness of the muscle layers in each stack by using the DAPI-labeled nuclei as an indication of the upper and lower limits of the muscle layers.

Measurement of Kit-positive ICC volume

The volumes of Kit-positive ICC were determined in 6 stacks from 14 *Htr2b*$^{+/+}$ and 14 *Htr2b*$^{-/-}$ ICC networks by 3-D reconstruction and volume rendering using Analyze™ running on a PC operating MS Windows, as previously described35. The volume quantification was done using unbiased thresholding algorithms to segment the images and determine the volume of Kit positive structures thereby minimizing any human influence in assessing the differences.

Primary culture of ICC from Neonatal Mice

ICC were cultured from dissociations of jejunal smooth muscle of 2–4 day old mice as previously described.18 Freshly dispersed cells were plated on 22-mm fibronectin-coated glass cover slips (Fisher Scientific) covered with mouse fibroblasts genetically engineered to

produce murine stem cell factor as previously described.36 Primary cell cultures were treated at 1h after plating and every 20h with the compounds as indicated, for 2.5 days, then fixed and labeled for Kit and Ki67.

Immunohistochemistry

Proliferating ICC in culture were identified by a standard procedure.18 Briefly, ICC were labeled for Kit immunoreactivity using ACK2 (1.65 μg mL^{-1} in 5% NDS). Dividing cells were identified by immunoreactivity for Ki67 (3 μg mL^{-1}). Kit-positive ICC and Ki67-positive proliferating ICC were counted using a BX51W1 upright fluorescence microscope (Olympus America Inc.). A 20X (0.5 NA) objective was used to count the number of Kit positive ICC with Ki67 positive nuclei in each field. One field covered 0.94 mm^2. At least 35 fields were counted per culture. Based on our previous studies, sampling from 35 fields gave an accurate measure of the mean density of the cells as that number of fields is sufficient to take into account variation in the cell density.

Transit Studies

We used red food dye as the gastrointestinal transit marker. Mice were briefly anesthetized using isofluorene. We passed red food dye into the stomach of the mice using a plastic gavage needle connected to a syringe with 100μl of the dye and waited for 30 min. After 30 min the mice were dissected and the transit time measured by the distance the dye has passed from the pylorus and expressed as the percentage of total length of small intestine (pylorus to cecum). Percentage transit time was measured in both *Htr2b*$^{-/-}$ and *Htr2b*$^{+/+}$ mice.

Chemicals

BW723C86 was purchased from Tocris Cookson Inc. (Ellisville, MO). BW723C86 (100mMolL^{-1}) stock solutions were made in DMSO. Further dilutions were made fresh on the experimental day in water, then added to the media. All dilutions were maintained in solution using a 37°C water bath. Red food dye was obtained from McCormick & Co., INC (Hunt Valley, MD).

Data Analysis

Statistical analysis was performed using the unpaired t test using a standard statistical software package (InStat 3; GraphPad software Inc., San Diego, CA). All data are expressed as the mean ± SEM where n represents the number of mice in each group for the data from the whole mounts and represents the number of separate dissociations for the cell culture data.

Results

The genotypes of all animals used in these experiments were determined using specific primers for the wild type and knockout alleles by PCR amplification from genomic DNA samples.

A proliferative response in ICC to application of the 5-HT_{2B} receptor agonists BW723C86 (10 nM) was not detected in cells derived from *Htr2b*$^{-/-}$ mice. In contrast to studies on ICC from BALB/c mice with no deficit in 5-HT_{2B} receptor signaling,18 application of the 5-HT_{2B} agonist had no effect on the number of Ki67 positive ICC after 20 h of treatment (proportion of Ki67-positive ICC: control; 15.13 ± 0.57 %, 10nM BW 13.01 ± 1.23 %; means for n = 4 dissociations for each treatment).

$5HT_{2B}$ Receptor is present in the $Htr2b^{+/+}$ adult mice

We looked for the presence of $5HT_{2B}$ receptor in the small intestinal sections of adult *Htr2b*$^{+/+}$ and *Htr2b*$^{-/-}$ mice. Cells from the ICC-DMP region were captured using the laser capture microdissection and RNA was isolated using the PicoPure RNA Isolation Kit. Using PCR, we showed that the β-Actin mRNA of expected size (151 bp) is expressed in the jejunum of both *Htr2b*$^{+/+}$ and *Htr2b*$^{-/-}$ adult mice (Fig 1A). $5HT_{2B}$ receptor mRNA of the expected size (375 bp) was amplified from the total RNA of the *Htr2b*$^{+/+}$ adult mice small intestine whereas it was not amplified in the *Htr2b*$^{-/-}$ adult mice small intestine (Fig 1B).

Proliferation of ICC occurs in vivo in the jejunum of adult

We first investigated whether we could detect Ki67-positive ICC in the jejunal muscle of 4 week old mice. Ki67-positive ICC were clearly identified by the positive labeling for Ki67 immunoreactivity in the nuclei of Kit-positive ICC in both the myenteric plexus (ICC-MY, Fig 2A) and deep muscular plexus (ICC-DMP) regions (Fig 2B). The apparent co-localization of Ki67 immunoreactivity with DAPI-labeling within the Kit-positive structures of the ICC was confirmed by 3-D reconstruction of the volume-rendered, confocal images stacks, as shown in the rotated, projection images (Fig 2C,D).

Proliferation of ICC is decreased in vivo in the myenteric plexus region of $Htr2b^{-/-}$ mice

We counted the number of Ki67–positive, proliferating ICC in both the myenteric plexus and deep muscular plexus regions in jejunal muscle preparations from adult *Htr2b*$^{+/+}$ and *Htr2b*$^{-/-}$ mice. In the myenteric plexus region, a total of 452 Ki67-positive ICC were counted from *Htr2b*$^{+/+}$ mice and 225 Ki67-positive ICC were counted from *Htr2b*$^{-/-}$ mice. The density of Ki67-positive ICC-MY region of whole mounts prepared from *Htr2b*$^{-/-}$ mice was 36% lower than in *Htr2b*$^{+/+}$ control mice (*Htr2b*$^{-/-}$ = 23 ± 2.75, *Htr2b*$^{+/+}$ = 37 ± 3.02 ICC per mm^2 of the whole mount, n = 14, mean ± SEM, $P < 0.05$, Fig. 3A, C) indicating that lack of $5\text{-}HT_{2B}$ receptor resulted in decreased proliferation of ICC-MY. There was no apparent difference in the number of Ki67-positive ICC-DMP (*Htr2b*$^{-/-}$ = 8.65 ± 0.94, *Htr2b*$^{+/+}$ = 8.25 ± 2.51 ICC per mm^2 of the whole mount, n = 14, $P > 0.05$) (Fig 3B, D). However, in the deep muscular plexus region, because of the lower density of ICC, only a total of 99 Ki67-positive ICC were counted from *Htr2b*$^{+/+}$ mice and 85 Ki67-positive ICC were counted from *Htr2b*$^{-/-}$ mice.

ICC network volumes are reduced in $Htr2b^{-/-}$ mice

We investigated whether loss of the $5\text{-}HT_{2B}$ receptor affected the volume of Kit-positive ICC-MY and ICC-DMP. The total volume of all Kit-positive ICC in *Htr2b*$^{-/-}$ mice was 34% lower when compared to the *Htr2b*$^{+/+}$ control mice (*Htr2b*$^{-/-}$ = 656579 ± 75788, *Htr2b*$^{+/+}$ = 989254 ± 66980 μm^3 per mm^2 of the whole mount, n = 14, $P < 0.05$). There was no difference between the overall thickness of the external muscle layers of *Htr2b*$^{-/-}$ and *Htr2b*$^{+/+}$ mice (*Htr2b*$^{-/-}$ = 19.1±1.98, *Htr2b*$^{+/+}$ = 14.6±1.14 μm, n = 14, mean ± SEM, $P > 0.05$). The difference in Kit-positive ICC volumes was seen for both the ICC-MY and the ICC-DMP. There was a 31% decrease in the volume of Kit-positive ICC-MY of *Htr2b*$^{-/-}$ mice when compared to the *Htr2b*$^{+/+}$ mice (*Htr2b*$^{-/-}$ = 522367 ± 64483, *Htr2b*$^{+/+}$ = 758091 ± 45553 μm^3 per mm^2 of the whole mount, n = 14, $P < 0.05$, Fig 4C). In the deep muscular plexus, there was a 42% decrease in the ICC-DMP network volume of the *Htr2b*$^{-/-}$mice when compared to the *Htr2b*$^{+/+}$ mice. (*Htr2b*$^{-/-}$ = 134212 ± 15455, *Htr2b*$^{+/+}$ = 231163 ± 25775 μm^3 per mm^2 of the whole mount, n = 14, $P < 0.05$, Fig 4D).

Number of ICC is lower in the deep muscular plexus region of $Htr2b^{-/-}$ mice

The impact of knocking out $5\text{-}HT_{2B}$ receptor expression on the number of ICC was determined by counting ICC-DMP. These cells were counted because, unlike the ICC-MY,

the ICC-DMP could be clearly quantified by looking at the number of DAPI-labeled nuclei within Kit positive structures with ICC-like morphology. There were 45% fewer ICC-DMP in the *Htr2b*$^{-/-}$ mice when compared to the *Htr2b*$^{+/+}$ mice. (*Htr2b*$^{-/-}$ = 301 ± 23, *Htr2b*$^{+/+}$ = 544 ± 42 ICC/mm^2, n = 14, P < 0.05, Fig 5B).

Intestinal transit

There was no difference in the gastrointestinal liquid transit time between the *Htr2b*$^{+/+}$ and *Htr2b*$^{-/-}$ (Percentage intestinal transit: *Htr2b*$^{+/+}$; 49.6 ± 1.86%, *Htr2b*$^{-/-}$; 40.7 ± 7.8%; P > 0.05, n = 5).

Discussion

In this study, we showed that ICC proliferate in the jejunum of adult mice and that lack of the 5-HT$_{2B}$ receptor *in vivo* was associated with decreased ICC proliferation in the myenteric plexus region, a reduced ICC network volume and a decrease in the number of ICC-DMP.

The detection of proliferating ICC in mature networks from adult mice by Ki67 immunolabeling confirms our preliminary work 37 and provides further evidence that mature ICC in mice divide as has been shown using different methods to label dividing ICC in 3 week old BALB/c mice.13 Proliferation of mature ICC was previously considered unlikely, but our data are consistent with increasing evidence for dynamic regulation of ICC numbers in adult mice. While 4 week old mice are adults, they are relatively young adults. Whether proliferation of ICC continues throughout adult life or decreases as the mice age is not known. A balance appears to exist between regeneration of ICC networks and loss of ICC.11 Proliferation of mature ICC and differentiation from stem cells38 contribute to ICC regeneration, whereas loss of ICC results from cell death 12 and trans- or de-differentiation. 39 The demonstration that knocking out expression of the 5-HT$_{2B}$ receptor and altering serotonin receptor signaling reduces the number of proliferating ICC adds further to our understanding of how this balance is regulated by humoral factors in the gastrointestinal tract.

Proliferating ICC were detected by using a monoclonal antibody to Ki67 protein in both the culture experiments on 3 day old pups as well as whole mount experiments in adult mice. Ki67 protein is present during all the active phases of cell cycle (G_1, S, G_2 and mitosis) and is absent in the resting cells (G_0). During the interphase stage, the antigen can be detected within the nucleus and during mitosis, the protein is relocated to the surface of the chromosomes40 making Ki67 a good marker for detecting proliferative cells.

The reduced number of proliferating ICC *in vivo* in *Htr2b*$^{-/-}$ mice compared to *Htr2b*$^{+/+}$ controls is consistent with our previous studies on ICC in primary culture.18 However, in that study, ICC were obtained from the jejunums of 3–5 day old mice, and the experiments carried out *ex vivo*, so it was necessary to investigate whether knockout of 5-HT$_{2B}$ receptor expression *in vivo* would affect more mature ICC networks. We determined in the current studies that there were fewer proliferating ICC in the mature myenteric plexus region of *Htr2b*$^{-/-}$ mice compared to *Htr2b*$^{+/+}$ mice, and that the impact of this decrease in proliferating ICC in the *Htr2b*$^{-/-}$ mice was a decrease in volume of the ICC networks. We also demonstrated a decrease in ICC numbers in the deep muscular plexus, a region where we could count the ICC. Unlike in the ICC-MY region, we did not detect a difference in the number of proliferating ICC in the ICC-DMP. This possibly reflects a lack of power and the challenge of obtaining a sufficient sample of dividing ICC from each tissue when both the frequency of cells and dividing cells is low. The resolution of the images was chosen to allow un-equivocal demonstration of the co-localization of Ki67 immunoreactivity to the

nuclei of Kit-positive ICC. This meant that despite collecting up to 12 fields (average size 255 × 255 μm) from 14 *Htr2b*$^{-/-}$ and 14 *Htr2b*$^{+/+}$ mice (330 total fields) we still did not have sufficient power to detect any less than a doubling in the number of proliferating ICC from the DMP. Because of this lack of power to detect a difference in proliferating ICC, the decrease in the number of ICC-DMP and the network volume cannot presently be directly attributed to changes in ICC proliferation due to loss of the 5HT$_{2B}$ receptor, although this remains a distinct possibility. On the other hand, the high density of ICC-MY compared to ICC-DMP meant that we had the power to detect the 36% decrease in proliferating ICC-MY.

The decrease in proliferating ICC-MY in the *Htr2b*$^{-/-}$ mice was associated with a decrease in volume of the ICC-MY networks. This difference is less than the more dramatic reduction in ICC networks that occur when Kit receptor signaling is abrogated such as in the white spotting and Steel Dickie mice 2, 41 or following inhibition of Kit receptor signaling.14 However the effect is similar to the reduction in Kit-positive ICC volumes reported for the stomachs of nNOS$^{-/-}$ mice.16 Despite the decrease in ICC network volumes, there was no difference in the gastrointestinal transit time between the *Htr2b*$^{+/+}$ and *Htr2b*$^{-/-}$ mice. This may reflect the fact that only liquid transit was measured as the mice were not certified as pathogen free and therefore we were unable to use the ^{13}C octanoic acid, gastric emptying of solids technique that we have previously used.42 Alternatively, the observed loss of ICC network volumes may be insufficient to cross a threshold where changes in gastrointestinal transit for liquids would become detectable.

Detection of an effect of 5-HT$_{2B}$ receptor knockout on ICC networks and numbers indicates that the receptor on ICC is activated *in vivo*. No other endogenous ligands are known to activate 5-HT$_{2B}$ receptors suggesting that 5-HT is available to activate these receptors *in vivo*. The source of the 5-HT is not clear. Serotonin is abundant in entero-endocrine cells in the mucosa of the gastrointestinal tract29, 30 and is produced by descending interneurons, 31, 32 although how much of this 5-HT is available outside the immediate environment of these cells is not known. Serotonin is also available from mast cells43, 44 and another potential source of 5-HT is the bloodstream where a large amount of the molecule is available from sequestered stores in platelets.25 There is no clear indication that either ICC-DMP or ICC-MY are preferentially affected by the loss of 5-HT$_{2B}$ receptors, so the differential distribution of those cells does not offer a clear clue as to which cells are closer to a source of 5-HT.

The presence of 5-HT$_{2B}$ receptors on ICC in adult mice, together with the functional evidence that these receptors directly change proliferation of ICC,18 leads us to strongly favor the conclusion that the decrease in ICC in *Htr2b*$^{-/-}$ mice was directly due to reduced 5-HT receptor-regulated proliferation in ICC. Other possibilities include an effect mediated through other cells such as smooth muscle and enteric nerves. 5-HT$_{2B}$ receptors, previously also known as 5-HT$_{2F}$ receptors, are present on gastric smooth muscle cells;45 however, 5-HT$_{2B}$ receptors have not been found on smooth muscle cells in the adult small intestine.46 5-HT$_{2B}$ receptor activation contributes to the development of enteric neurons in fetal mice, 46 but there is little effect of loss of 5-HT$_{2B}$ receptors on adult enteric nerves except for a decrease in the number of serotonergic neurons in the myenteric plexus (Dr. Gershon unpublished data). Given that serotonergic neurons are primarily descending inhibitory interneurons in the gut and represent less than 3% of all enteric neurons, it is unlikely that these differences can account for the observed changes in ICC proliferation. It is possible that loss of 5-HT$_{2B}$ receptors on neurons or other cell types might also influence the development of ICC networks independently from the direct reduction in ICC proliferation.

In conclusion, this study demonstrates that 5-HT_{2B} receptor signaling is an important part of the balance of factors that regulate ICC network volume and ICC numbers. Targeting 5-HT availability may have the potential to protect ICC networks from injury or can assist in repairing ICC networks after injury.

Acknowledgments

The authors would like to thank Mr. Gary Stoltz for tissue dissection, Mr. Peter Strege for help with the figures and Ms. Kristy Zodrow for secretarial assistance. This work was supported and funded by NIH DK57061 (GF) and NS12969 (MDG) and from the Centre National de la Recherche Scientifique, the Institut National de la Santé et de la Recherche Médicale, the Université Pierre et Marie Curie, and by grants from the Fondation de France, the Fondation pour la Recherche Médicale, the Association pour la Recherche contre le Cancer, the French ministry of research (Agence Nationale pour la Recherche), the Federation des Maladies Orphelines, and the European Union (LM).

References

1. Barajas-Lopez C, Berezin I, Daniel EE, Huizinga JD. Pacemaker activity recorded in interstitial cells of Cajal of the gastrointestinal tract. Am J Physiol. 1989; 257:C830–5. [PubMed: 2801932]
2. Ward SM, Burns AJ, Torihashi S, Sanders KM. Mutation of the proto-oncogene c-kit blocks development of interstitial cells and electrical rhythmicity in murine intestine. J Physiol. 1994; 480:91–7. [PubMed: 7853230]
3. Ward SM, Beckett EA, Wang X, Baker F, Khoyi M, Sanders KM. Interstitial cells of Cajal mediate cholinergic neurotransmission from enteric motor neurons. J Neurosci. 2000; 20:1393–403. [PubMed: 10662830]
4. Burns AJ, Lomax AE, Torihashi S, Sanders KM, Ward SM. Interstitial cells of Cajal mediate inhibitory neurotransmission in the stomach. Proc Natl Acad Sci U S A. 1996; 93:12008–13. [PubMed: 8876253]
5. Strege PR, Holm AN, Rich A, et al. Cytoskeletal modulation of sodium current in human jejunal circular smooth muscle cells. Am J Physiol Cell Physiol. 2003; 284:C60–6. [PubMed: 12475760]
6. Won KJ, Sanders KM, Ward SM. Interstitial cells of Cajal mediate mechanosensitive responses in the stomach. Proc Natl Acad Sci U S A. 2005; 102:14913–8. [PubMed: 16204383]
7. Farrugia G, Lei S, Lin X, et al. A major role for carbon monoxide as an endogenous hyperpolarizing factor in the gastrointestinal tract. Proc Natl Acad Sci U S A. 2003; 100:8567–70. [PubMed: 12832617]
8. Vittal H, Farrugia G, Gomez G, Pasricha PJ. Mechanisms of disease: the pathological basis of gastroparesis--a review of experimental and clinical studies. Nat Clin Pract Gastroenterol Hepatol. 2007; 4:336–46. [PubMed: 17541447]
9. He CL, Burgart L, Wang L, et al. Decreased interstitial cell of cajal volume in patients with slow-transit constipation. Gastroenterology. 2000; 118:14–21. [PubMed: 10611149]
10. Lyford GL, He CL, Soffer E, et al. Pan-colonic decrease in interstitial cells of Cajal in patients with slow transit constipation. Gut. 2002; 51:496–501. [PubMed: 12235070]
11. Farrugia G. Interstitial cells of Cajal in health and disease. Neurogastroenterol Motil. 2008; 20 (Suppl 1):54–63. [PubMed: 18402642]
12. Gibbons SJ, De Giorgio R, Pellegrini MS, et al. Apoptotic cell death of human interstitial cells of Cajal. Neurogastroenterol Motil. 2009; 21:85–93. [PubMed: 18798796]
13. Mei F, Zhu J, Guo S, et al. An age-dependent proliferation is involved in the postnatal development of interstitial cells of Cajal in the small intestine of mice. Histochem Cell Biol. 2009; 131:43–53. [PubMed: 18836738]
14. Maeda H, Yamagata A, Nishikawa S, Yoshinaga K, Kobayashi S, Nishi K. Requirement of c-kit for development of intestinal pacemaker system. Development. 1992; 116:369–75. [PubMed: 1283735]
15. Horvath VJ, Vittal H, Ordog T. Reduced insulin and IGF-I signaling, not hyperglycemia, underlies the diabetes-associated depletion of interstitial cells of Cajal in the murine stomach. Diabetes. 2005; 54:1528–33. [PubMed: 15855342]

16. Choi KM, Gibbons SJ, Roeder JL, et al. Regulation of interstitial cells of Cajal in the mouse gastric body by neuronal nitric oxide. Neurogastroenterol Motil. 2007; 19:585–95. [PubMed: 17593140]
17. Choi KM, Gibbons SJ, Nguyen TV, et al. Heme oxygenase-1 protects interstitial cells of Cajal from oxidative stress and reverses diabetic gastroparesis. Gastroenterology. 2008; 135:2055–64. 64, e1–2. [PubMed: 18926825]
18. Wouters MM, Gibbons SJ, Roeder JL, et al. Exogenous serotonin regulates proliferation of interstitial cells of Cajal in mouse jejunum through 5-HT2B receptors. Gastroenterology. 2007; 133:897–906. [PubMed: 17854596]
19. Horvath VJ, Vittal H, Lorincz A, et al. Reduced stem cell factor links smooth myopathy and loss of interstitial cells of cajal in murine diabetic gastroparesis. Gastroenterology. 2006; 130:759–70. [PubMed: 16530517]
20. Gershon MD, Tack J. The serotonin signaling system: from basic understanding to drug development for functional GI disorders. Gastroenterology. 2007; 132:397–414. [PubMed: 17241888]
21. Banasr M, Hery M, Printemps R, Daszuta A. Serotonin-induced increases in adult cell proliferation and neurogenesis are mediated through different and common 5-HT receptor subtypes in the dentate gyrus and the subventricular zone. Neuropsychopharmacology. 2004; 29:450–60. [PubMed: 14872203]
22. Huang GJ, Herbert J. The role of 5-HT1A receptors in the proliferation and survival of progenitor cells in the dentate gyrus of the adult hippocampus and their regulation by corticoids. Neuroscience. 2005; 135:803–13. [PubMed: 16129565]
23. Cattaneo MG, Fesce R, Vicentini LM. Mitogenic effect of serotonin in human small cell lung carcinoma cells via both 5-HT1A and 5-HT1D receptors. Eur J Pharmacol. 1995; 291:209–11. [PubMed: 8566173]
24. Abdouh M, Albert PR, Drobetsky E, Filep JG, Kouassi E. 5-HT1A-mediated promotion of mitogen-activated T and B cell survival and proliferation is associated with increased translocation of NF-kappaB to the nucleus. Brain Behav Immun. 2004; 18:24–34. [PubMed: 14651944]
25. Lesurtel M, Graf R, Aleil B, et al. Platelet-derived serotonin mediates liver regeneration. Science. 2006; 312:104–7. [PubMed: 16601191]
26. Nebigil CG, Jaffre F, Messaddeq N, et al. Overexpression of the serotonin 5-HT2B receptor in heart leads to abnormal mitochondrial function and cardiac hypertrophy. Circulation. 2003; 107:3223–9. [PubMed: 12810613]
27. De Lucchini S, Ori M, Cremisi F, Nardini M, Nardi I. 5-HT2B-mediated serotonin signaling is required for eye morphogenesis in Xenopus. Mol Cell Neurosci. 2005; 29:299–312. [PubMed: 15911353]
28. Fiorica-Howells E, Maroteaux L, Gershon MD. 5-HT2B receptors are expressed by neuronal precursors in the enteric nervous system of fetal mice and promote neuronal differentiation. Ann N Y Acad Sci. 1998; 861:246. [PubMed: 9928269]
29. Erspamer V. Pharmacology of indole-alkylamines. Pharmacol Rev. 1954; 6:425–87. [PubMed: 13236482]
30. Bertrand PP. Real-time measurement of serotonin release and motility in guinea pig ileum. J Physiol. 2006; 577:689–704. [PubMed: 16959854]
31. Young HM, Furness JB. Ultrastructural examination of the targets of serotonin- immunoreactive descending interneurons in the guinea pig small intestine. J Comp Neurol. 1995; 356:101–14. [PubMed: 7629305]
32. Costa M, Brookes SJ, Steele PA, Gibbins I, Burcher E, Kandiah CJ. Neurochemical classification of myenteric neurons in the guinea-pig ileum. Neuroscience. 1996; 75:949–67. [PubMed: 8951887]
33. Nebigil CG, Choi DS, Dierich A, et al. Serotonin 2B receptor is required for heart development. Proc Natl Acad Sci U S A. 2000; 97:9508–13. [PubMed: 10944220]
34. Sanders KM, Ordog T, Koh SD, Torihashi S, Ward SM. Development and plasticity of interstitial cells of Cajal. Neurogastroenterol Motil. 1999; 11:311–38. [PubMed: 10520164]

35. Miller SM, Farrugia G, Schmalz PF, Ermilov LG, Maines MD, Szurszewski JH. Heme oxygenase 2 is present in interstitial cell networks of the mouse small intestine. Gastroenterology. 1998; 114:239–44. [PubMed: 9453482]
36. Rich A, Miller SM, Gibbons SJ, Malysz J, Szurszewski JH, Farrugia G. Local presentation of Steel factor increases expression of c-kit immunoreactive interstitial cells of Cajal in culture. Am J Physiol Gastrointest Liver Physiol. 2003; 284:G313–20. [PubMed: 12388202]
37. Tharayil, V.; Wouters, M.; Stanich, J., et al. Proliferation of Interstitial cells of Cajal occurs in Adult Mice and is dependent on 5HT2B Receptors and Protein Kinase gamma. In: Rustgi, A., editor. Digestive Disease Week. Chicago: Gastroenterology; 2009.
38. Lorincz A, Redelman D, Horvath VJ, Bardsley MR, Chen H, Ordog T. Progenitors of interstitial cells of cajal in the postnatal murine stomach. Gastroenterology. 2008; 134:1083–93. [PubMed: 18395089]
39. Torihashi S, Nishi K, Tokutomi Y, Nishi T, Ward S, Sanders KM. Blockade of kit signaling induces transdifferentiation of interstitial cells of cajal to a smooth muscle phenotype. Gastroenterology. 1999; 117:140–8. [PubMed: 10381920]
40. Scholzen T, Gerdes J. The Ki-67 protein: from the known and the unknown. J Cell Physiol. 2000; 182:311–22. [PubMed: 10653597]
41. Mikkelsen HB, Malysz J, Huizinga JD, Thuneberg L. Action potential generation, Kit receptor immunohistochemistry and morphology of steel-Dickie (Sl/Sld) mutant mouse small intestine. Neurogastroenterol Motil. 1998; 10:11–26. [PubMed: 9507248]
42. Choi KM, Zhu J, Stoltz GJ, et al. Determination of gastric emptying in nonobese diabetic mice. Am J Physiol Gastrointest Liver Physiol. 2007; 293:G1039–45. [PubMed: 17884976]
43. De Clerck F, Somers Y, Van Gorp L, Xhonneux B. Platelet activation by endogenous 5-hydroxytryptamine and histamine released by mast cell degranulation with compound 48/80 in the rat. Agents Actions. 1983; 13:81–7. [PubMed: 6858790]
44. Kushnir-Sukhov NM, Brown JM, Wu Y, Kirshenbaum A, Metcalfe DD. Human mast cells are capable of serotonin synthesis and release. J Allergy Clin Immunol. 2007; 119:498–9. [PubMed: 17291861]
45. Wainscott DB, Cohen ML, Schenck KW, et al. Pharmacological characteristics of the newly cloned rat 5-hydroxytryptamine2F receptor. Mol Pharmacol. 1993; 43:419–26. [PubMed: 8450835]
46. Fiorica-Howells E, Maroteaux L, Gershon MD. Serotonin and the 5-HT(2B) receptor in the development of enteric neurons. J Neurosci. 2000; 20:294–305. [PubMed: 10627607]

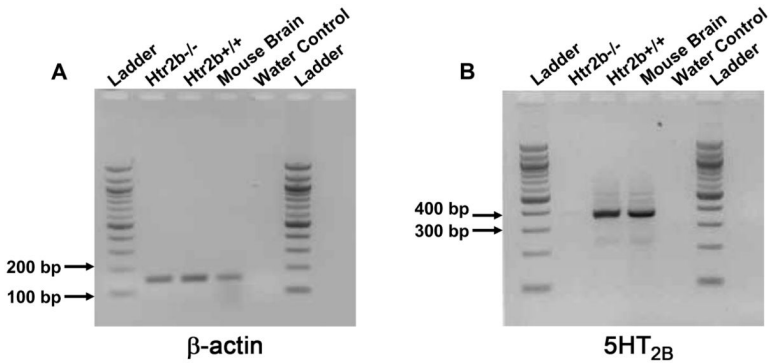

Fig 1. Expression of 5HT2B receptors in adult mouse small intestinal circular muscle layer

(A) The expected PCR product size (151 bp) for β-Actin mRNA was amplified in adult mouse jejunum of both *Htr2b*$^{-/-}$ and *Htr2b*$^{+/+}$ mice. Mouse brain was used as positive control. (B) 5HT2B mRNA is expressed in the adult mouse jejunum of *Htr2b*$^{+/+}$ mice and is absent in the *Htr2b*$^{-/-}$ adult mouse jejunum. Ladder: 100 base pair DNA ladder (NEB).

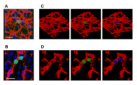

Fig 2. Identification of Ki67-positive, proliferating ICC in the adult mouse jejunum

(A) Projection image from a region of a confocal image stack showing colocalization of Ki67 immunoreactivity (green) with DAPI (cyan) in a Kit-positive (red) ICC-MY. (B) Similar image showing a Ki67- positive ICC-DMP (C) Volume rendered, 3-D bitmaps of the positively labeled voxels in (A), rotated to demonstrate the labeling more clearly showing the ICC network (red), with Ki67 labeling (green) and with DAPI (cyan). (D) Bitmap of the positively labeled voxels in (B). Scale bars 20μm.

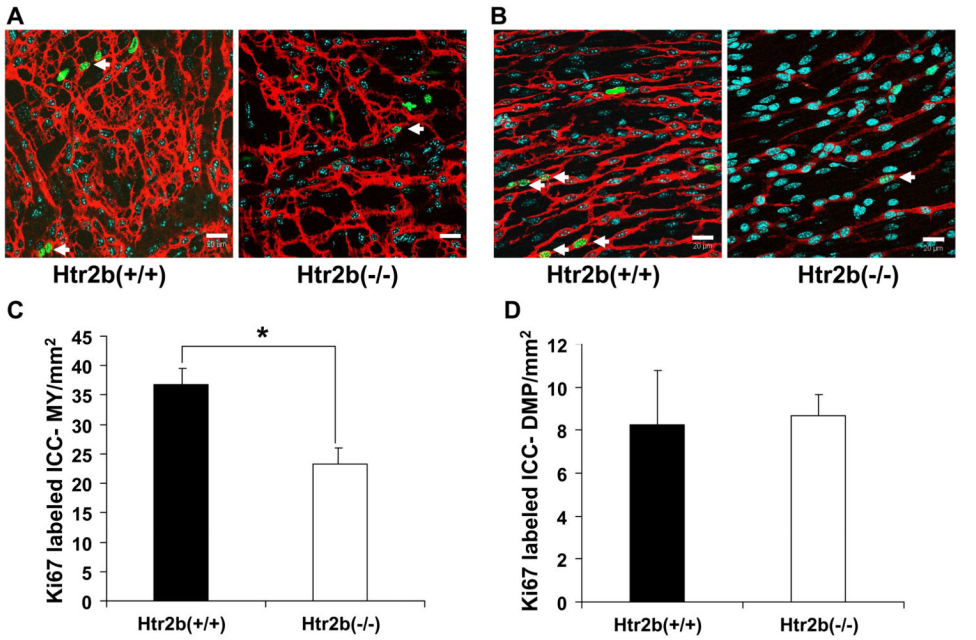

Fig 3. Number of proliferating ICC is altered in the myenteric plexus (MY) region but not in the deep muscular plexus (DMP)

Panels A and B show single confocal image slices (0.3 μm thick) with Ki67-positive (green) nuclei (cyan) of dividing cells and the Kit labeled (red) ICC networks in whole mounts from the jejunum. (A) Images from the MY region of 4 week old, *Htr2b*$^{+/+}$ (left) and *Htr2b*$^{-/-}$ mice (right). (B) Images from the DMP region of 4 week old, *Htr2b*$^{+/+}$ (left) and *Htr2b*$^{-/-}$ mice (right). Scale bars 20μm. Arrows in panels A and B mark the proliferating cells that were Kit-positive. (C) Quantification of the proliferating ICC-MY scaled to give the number through the whole thickness of a 1 mm^2 area of the tissue. (D) Data from the DMP region represented in the same manner. Data are expressed as mean ±SEM; * $P < 0.05$ by unpaired t-test, n = 14 mice.

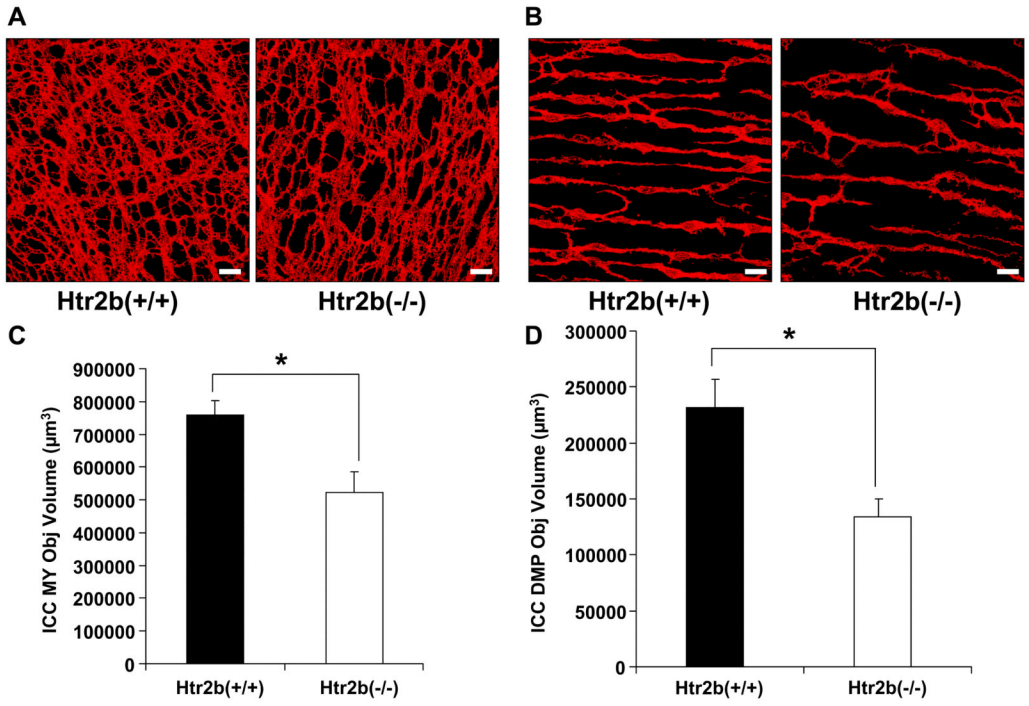

Fig 4. The volume of both myenteric plexus ICC (ICC-MY) and deep muscular plexus ICC (ICC-DMP) networks is reduced in *Htr2b*$^{-/-}$ mice

Volume rendered, 3-D bitmaps of the Kit-positive ICC network in 4 week old, *Htr2b*$^{+/+}$ (left) and *Htr2b*$^{-/-}$ mice (right) of (A) the MY region and (B) the DMP region. Scale bars 20µm. (C) Quantification of the Kit-positive ICC-MY volume scaled to give the volume through the whole thickness of a 1 mm^2 area of the myenteric plexus region. (D) Quantification of the Kit-positive ICC-DMP volume scaled to give the volume through the whole thickness of a 1 mm^2 area of the deep muscular region. Data are expressed as mean ±SEM; * $P < 0.05$ by unpaired t-test, n = 14 mice.

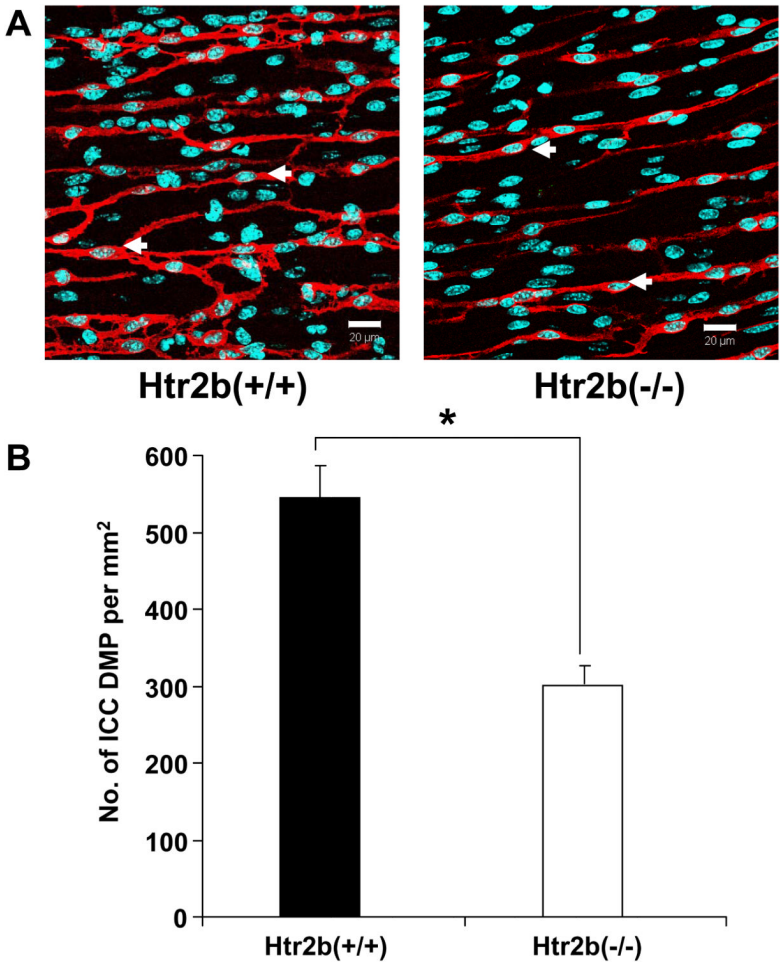

Fig 5. The number of deep muscular plexus ICC (ICC-DMP) is reduced in *Htr2b*$^{-/-}$ Mice

(A) Single confocal image slices (0.3 µm thick) showing the nuclei (cyan) of all cells and the Kit labeled (red) ICC-DMP region of 4 week old, *Htr2b*$^{+/+}$ (left) and *Htr2b*$^{-/-}$ mice (right). Scale bars 20µm. (B) Quantification of the ICC-DMP numbers scaled to give the number of cells through the whole thickness of a 1 mm^2 area of the deep muscular region. Data are expressed as mean ±SEM; * $P < 0.05$ by unpaired t-test, n = 14 mice.

Table 1

Primer sequences and their optimized melting temperature (Tm) and extension times

	Primer Sequence	Tm (°C)	Extension Time (Sec)	Length Amplicon (nt)
$5HT_{2B}$	5′ – AAGCCAATTCAGGCCAATC	62	30	504
	3′ – GGGCACCACATAAGCAGAAA			
$5HT_{2B}$ nested	5′ – ATTCAGGCCAATCAGTGCAA	60	30	375
	3′ – CTGTGAGACCCATCCAGCAT			
β-actin	5′ – ATGGTGGGAATGGGTCAGAAGG	56	30	151
	3′ - GCTCATTGTAGAAGGTGTGGTGCC			